Microfluid Nanofluid (2012) 13:909–917
DOI 10.1007/s10404-012-1009-4

RESEARCH PAPER

Fluorescence-profile pre-definable quantum-dot barcodes in liquid-core microcapsules

Bo Wu · Hai-Qing Gong

Received: 16 April 2012 / Accepted: 28 May 2012 / Published online: 1 August 2012

Abstract Microparticles incorporated with quantum-dot (QD) barcodes for multiplexed bioassays attract a great attention due to their potential applications in drug discovery, gene profiling and clinic diagnostics. However, the existing QD barcodes lack a necessary optical stability to ambient fluids or a repeatability of fluorescent profiles. We developed a new QD barcode by loading an aqueous QD mixture as a liquid core into a monodispersed polymer microcapsule by a microfluidic method to avoid those problems. We found that the QDs in the liquid cores were able to maintain their original characteristics, especially the linear relation between photoluminescence intensity and concentration. In addition, we found that the fluorescent profiles of the QD-loaded liquid cores were the same as those of the QD mixtures before being loaded inside the microcapsules. With these two properties, the QD barcodes can be predefined directly by multiplexing the emission peaks and concentrations of the QDs in the liquid cores. Furthermore, the graphical information from fluorescent images of the microcapsules, such as the sizes and numbers of the QD-loaded liquid cores, offers another dimension for barcoding to increase the coding capacity. We also presented a microfluidic method to manufacture the QD-barcoded microcapsules of size ~ 30 μm. These predefinable QD barcodes with stable fluorescent profiles can be used as a platform for various high-throughput screening applications in different bioassay buffers.

B. Wu · H.-Q. Gong (✉)
School of Mechanical and Aerospace Engineering, Nanyang Technological University, 50 Nanyang Avenue, Singapore 639798, Singapore
e-mail: MHQGONG@ntu.edu.sg

Keywords Microcapsule · Double emulsion · Quantum dot · Barcode

1 Introduction

Modern biological and medical research in gene expression profiling, drug discovery and clinical diagnostics requires high-throughput, flexible and low-cost methods for multiplexed assays. Microparticles labeled with specific barcodes receive great attention for these applications, due to their ability to carry different probe molecules to conduct multiplexed assays by tracking their barcodes (Wilson et al. 2006; Cederquist et al. 2010; Birtwell and Morgan 2009). The barcodes can be formed by graphical hollow (Pregibon et al. 2007) or chromatic (Lee et al. 2010) patterns and fluorescence emissions (Fulton et al. 1997; Kellar and Iannone 2002), as well as using Raman spectra (Su et al. 2004), rare earth elements (Dejneka et al. 2003), metallic patterns (Nicewarner-Peña et al. 2001), photo crystals (Zhao et al. 2009), DNA-based monomers (Lee et al. 2009), magnetic elements (Hayward et al. 2010) and holograms (Birtwell et al. 2008). Particularly, the QD barcodes can be created with a high coding capacity by multiplexing fluorescence colors and intensity levels of QD-incorporated microparticles (Han et al. 2001).

In the current state of the art, three methods are developed to incorporate the QDs into the microparticles for barcoding: (1) embedding the QDs at the outer layers of microparticles (Han et al. 2001; Gao and Nie 2004) as illustrated in Fig. 1a; (2) coating the QDs over the outer surfaces of microparticles by charged polyelectrolyte layers (Wang et al. 2002; Rauf et al. 2009) as illustrated in Fig. 1b; (3) doping the QDs inside the polymer microparticles (Zhao et al. 2011; Fournier-Bidoz et al. 2008)

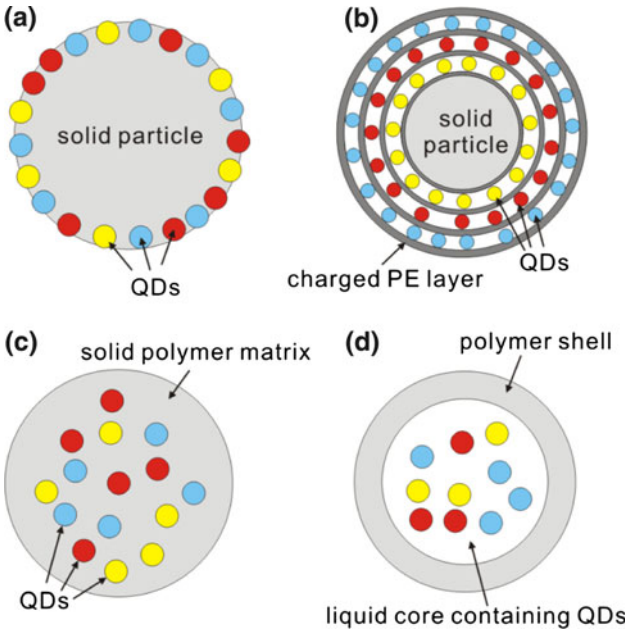

Fig. 1 Schematic illustration of the QD barcodes. **a** A microparticle embedded with the QDs at the outer surface. **b** A microparticle coated with the QDs over the outer surface. **c** A microparticles doped with the QDs inside the solid polymer matrix. **d** A QD-barcoded liquid-core microcapsule in which a QD-loaded liquid core is protected by a rigid polymer shell

as illustrated in Fig. 1c. The QD barcodes made by embedding or coating the QDs at the outer surface of microparticles have drawbacks such as the leakage of QDs and the changes of QD photoluminescence emissions in different bioassay buffers (Lee et al. 2007). Taking advantages of microfluidic techniques, monodispersed microparticles are made from the QD-mixed polymer precursor in a high production rate with low costs (Fournier-Bidoz et al. 2008). The QDs are doped inside the microparticles in a high volume fraction without leakage. However, due to the shrinkage of solidified polymer precursor (Lee et al. 2007) and Förster resonance energy transfer (FRET) of the aggregated QDs in the polymer matrix (Vaidya et al. 2007), the fluorescent spectra of these QD-doped microparticles become different from those of the QD mixtures before being doped inside the solid-state polymer matrix. The microparticles doped with different QD mixtures may have similar fluorescent profiles. As a result, the fluorescent profiles of the QD-doped microparticles have to be interrogated to check their specificities to form unique barcodes. Moreover, the fluorescent profiles of the microparticles doped with an identical QD mixture lack a necessary repeatability because of these unpredictable changes of QD photoluminescence emissions in the polymer matrix.

We developed a new QD liquid-core barcode by loading an aqueous QD mixture as a liquid core into a transparent polymer shell to form a microcapsule, as illustrated in Fig. 1d. The microcapsules used for barcoding are templated from water-in-oil-in-water (W/O/W) double-emulsion droplets (Okushima et al. 2004; Nie et al. 2005; Utada et al. 2005) in a microfluidic liquid-core barcode generator, which consists of a T-shape junction and a flow-focusing junction to form the liquid cores and the double-emulsion droplets, respectively. Compared with the barcodes made by embedding or coating the QDs at the outer surfaces of microparticles, the liquid-core barcode has a stable fluorescence profile in different bioassay buffers, since the QDs in the liquid core are separated from the ambient fluids by the rigid polymer shell. Compared with the barcode made by doping the QDs inside the microparticle, the liquid-core barcode can be predefined directly by the composition of the QD mixture, because the QDs in the liquid core maintain their original characteristics including the linear relation between QD photoluminescence intensity and concentration. Therefore, the liquid-core barcodes can be simply formed by multiplexing the QD emission peaks and concentrations in the liquid cores of the microcapsules. Furthermore, the graphical information from the fluorescent micrographs such as the sizes and numbers of the QD-loaded liquid cores in individual microcapsules offers another dimension for barcoding to increase the coding capacity.

2 Experimental

2.1 Design of liquid-core barcode generator

The microfluidic network of the liquid-core barcode generator is illustrated in Fig. 2a. The microcapsules are formed in a three-step process. Firstly, droplets of the aqueous QD mixture are generated at the T-shape junction and suspended in a flow of a polymer precursor of ethoxylated trimethylolpropane triacrylate (ETPTA) (Fig. 2b). Secondly, the QD-mixture droplets are engulfed by globules of the ETPTA polymer precursor to form the W/O/W double-emulsion droplets in a flow of sodium dodecyl sulfate (SDS) solution at the flow-focusing junction (Fig. 2c). Finally, the ETPTA globules are cured by UV light as the polymer shells to form the microcapsules in a serpentine channel (Fig. 2d). The aqueous QD mixture, the polymer precursor of ETPTA and the SDS solution are the inner-phase fluid, the middle-phase fluid and the outer-phase fluid of the W/O/W double emulsion, respectively. To form the W/O/W double emulsion, the serpentine channel downstream of the flow-focusing junction is patterned to be hydrophilic and the other channels are hydrophobic. To suspend the double-emulsion droplets spherically in the flow of SDS solution, the serpentine channel should be made with a square cross section.

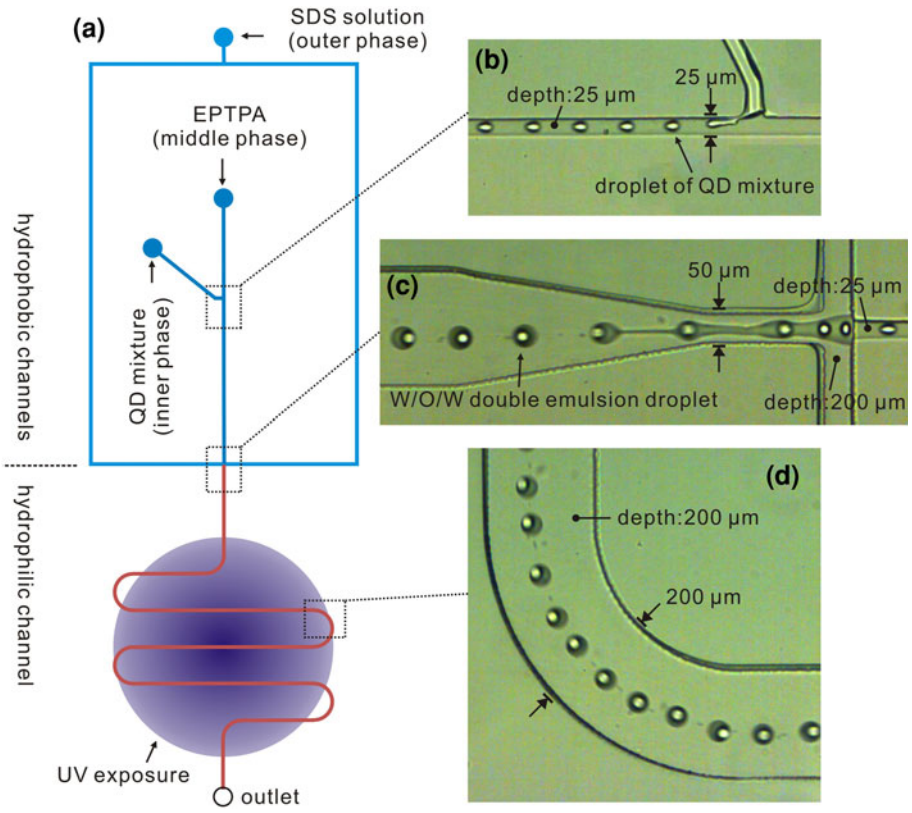

Fig. 2 **a** Schematic diagram of the liquid-core barcode generator. **b** T-shape junction to form the droplets of aqueous QD mixture. **c** Flow-focusing junction to form the W/O/W double emulsion. **d** The double-emulsion droplets queue in a line in the serpentine channel. The polymer precursor globules of ETPTA are cured by UV light to form the microcapsules in the serpentine channel. The dimensions of the channels are labeled in (**b**) ~ (**d**)

2.2 Fabrication of liquid-core barcode generator

Firstly, a mold of the microfluidic network was made on a piece of silicon wafer by photolithography of SU-8 photoresists. Two alignment marks were made on the silicon wafer by deep reactive-ion etching (Fig. 3a). Then, a SU-8 microstructure of the microfluidic network was made at a height of 25 μm on the silicon wafer with the two alignment marks as the first layer of the mold (Fig. 3b). Another SU-8 microstructure of the serpentine channel was made at a height of 175 μm above the first-layer microstructure with the two alignment marks to form the second layer of the mold (Fig. 3c).

Secondly, the microfluidic network was made by soft lithography of polydimethylsiloxane (PDMS) (Sylgard 184, Dow Corning, USA). PDMS base was mixed with its curing agent in a ratio of 10:1 (w/w) and degassed before being poured on the mold. After curing at 80 °C for 4 h in an oven, the cured PDMS cast was peeled off from the mold (Fig. 3d). To assemble the liquid-core barcode generator, the cured PDMS cast was bonded covalently to a PDMS thin film coated on a piece of acrylic (PMMA) substrate by oxygen plasma (Fig. 3e). Then, the generator was placed in the oven at 80 °C for 3 days to reverse the original hydrophobic surface of PDMS.

Thirdly, the hydrophobic PDMS serpentine channel was patterned to be hydrophilic by UV-initiated graft polymerization of poly(acrylic acid) (PAA) (Schneider et al. 2010). A photoinitiator (PI) solution of 10 % (v/v) 2-hydroxy-2-methylpropiophenone (Daracure 1173) in acetone was flushed through the microfluidic network (Fig. 3f). After 10 min, the PI solution in the channels was removed by air and the channels were dried by vacuum for 10 min. Then these channels were filled with a monomer solution of 10 % (v/v) acrylic acid (AA) in deionized water (Fig. 3g). To graft PAA at the PDMS inner wall, the serpentine channel was exposed to UV light from a mercury lamp of a microscope (LV-100, Nikon, Japan) (Fig. 3h). The region above the other channels was covered by a piece of aluminum foil to avoid UV exposure. Finally, the microfluidic network was flushed by ethanol for 30 min and water at pH 10 (adjusted by 1 M NaOH solution) for another 30 min to remove the unreacted AA (Fig. 3i).

2.3 Liquid-core barcode formation

The inner-phase fluid was prepared by dispersing carboxyl-functionalized CdTe QDs (PlasmaChem, Germany) in deionized water. The QD emission peaks are at 550, 600 and 650 nm, respectively. The molar concentrations of the QDs were measured and calibrated based on Lambert–Beer's law with an empirical equation of determining the CdTe QD extinction coefficients at their first excitons (Yu et al. 2003). The QD absorbances were measured by a

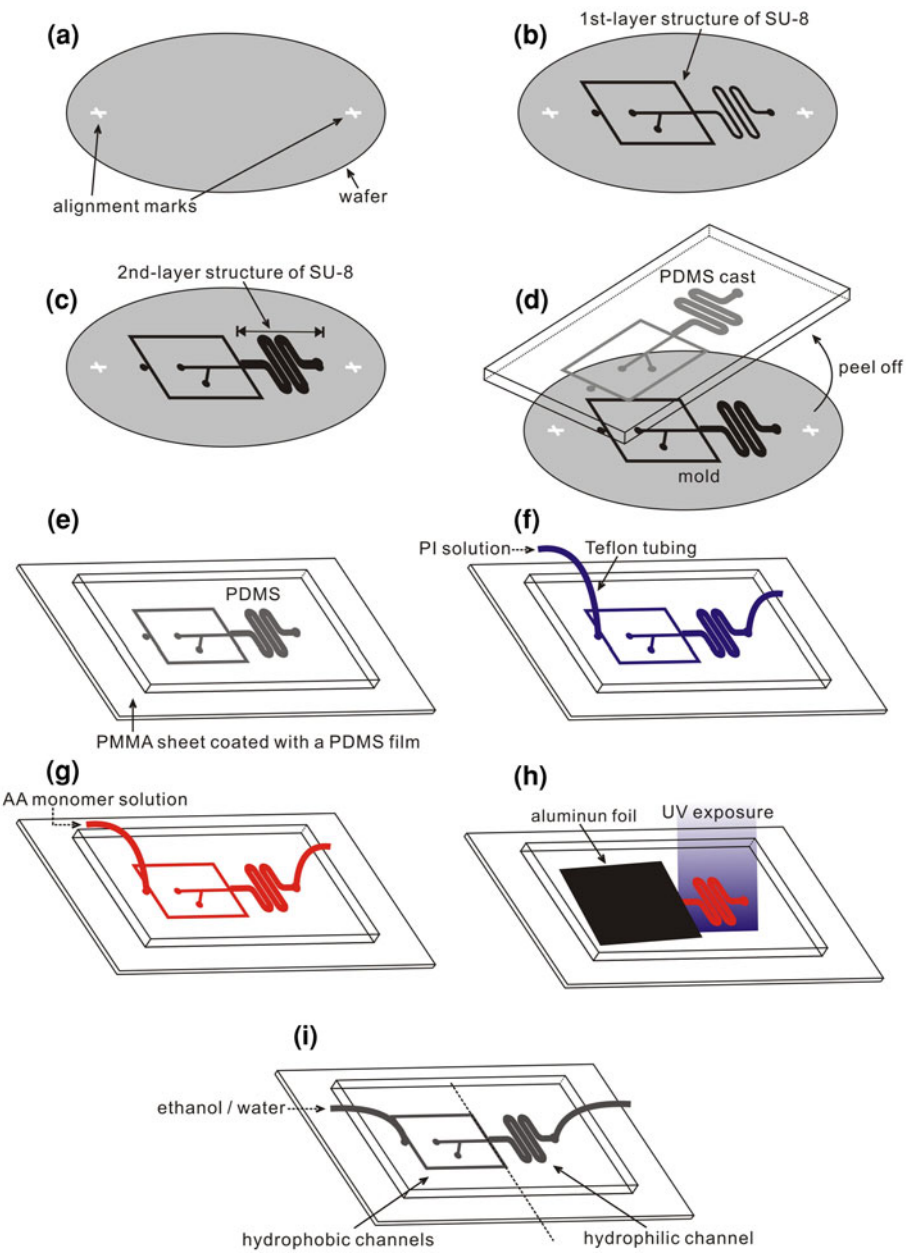

Fig. 3 Schematic illustration of the fabrication of liquid-core barcode generator. **a** Two alignment marks were made on a silicon wafer by DIRE. **b** First-layer SU-8 microstructure of the microfluidic network was made on the silicon wafer. **c** Second-layer SU-8 microstructure of the serpentine section was made above the first-layer microstructure. **d** Soft lithography of PDMS on the mold. **e** The cured PDMS cast was bonded covalently to a PDMS thin film coated on a PMMA substrate by oxygen plasma. **f** The channels of the microfluidic network were flushed by PI solution for 10 min. **g** The channels were filled with AA monomer solution. **h** The serpentine channel was exposed to UV light to graft PAA on the PDMS inner wall. The other channels were covered by a piece of aluminum foil to avoid UV exposure. **i** The microfluidic network was flushed by ethanol for 30 min and water at pH 10 for another 30 min

UV–VIS spectrophotometer (UV-2450, SHIMADZU, Japan). The middle-phase fluid was the ETPTA polymer precursor added with 2 % (w/v) photoinitiator of Daracure 1173 and 4 % (w/v) surfactant of sorbitan monooleate (Span 80). The outer-phase fluid was prepared by adding 2 % (w/w) SDS in deionized water. The three fluids of the W/O/W double emulsion were injected into the liquid-core barcode generator by three syringe pumps (F-100, Chemyx, USA) independently. The ETPTA globules of the double-emulsion droplets were cured to form the microcapsules in the serpentine channel by UV light from a mercury lamp equipped to an inverted microscope (Eclipse T*i*, Nikon, Japan).

2.4 Characterization

The droplet generation processes at the T-shape junction and the flow-focusing junction were observed and recorded by a high speed camera (Fastcam APX-RS, Photron, Japan) mounted to the inverted microscope. The bright-field micrographs of the microcapsules were captured by a monochromatic CCD camera (RETIGE EX*i*, Qimaging, Canada) mount on the microscope. The fluorescent micrographs of the microcapsules were captured by the monochromatic CCD camera with three narrow bandpass optical filters (Thorlabs, USA) under UV excitation (325 ~ 375 nm). The center wavelengths of these optical

filters are at 550, 600 and 650 nm, respectively, with FWHM of 10 nm. The fluorescent spectra of the QD-barcoded microcapsules were recorded by a laser scanning confocal microscope (LSM710, Carl Zeiss, Germany) with the hyperspectral imaging function.

3 Results and discussion

3.1 Microfluidic operation

The monodispersed microcapsules with the liquid cores were templated from the W/O/W double-emulsion droplets in the liquid-core barcode generator. This microfluidic method allows the formation of the microcapsules within narrow size distributions (less than 3 %) for both of the liquid cores and the polymer shells. These monodispersed microcapsules can create more barcodes than the polydispersed microparticles encoded by a ratiometric algorithm (Eastman et al. 2006; Lee et al. 2007). The sizes of the liquid cores and polymer shells can be controlled independently by the flow rates of the double-emulsion. As shown in Fig. 4, the double-emulsion droplets of size 34.2 μm were formed with the liquid cores in two different sizes by changing the ratio of the inner-phase flow rate (Q_i) to the middle-phase flow rate (Q_m), while the out-phase flow rate (Q_o) was set constantly. Furthermore, the numbers of liquid cores in individual double-emulsion droplets can be controlled by the ratio of the droplet generation frequency at the T-shape junction to the double-emulsion generation frequency at the flow-focusing junction. As shown in Fig. 5, each double-emulsion droplet was formed with two liquid cores. The microcapsules made with the liquid cores in different sizes and two liquid cores are shown in Fig. 6.

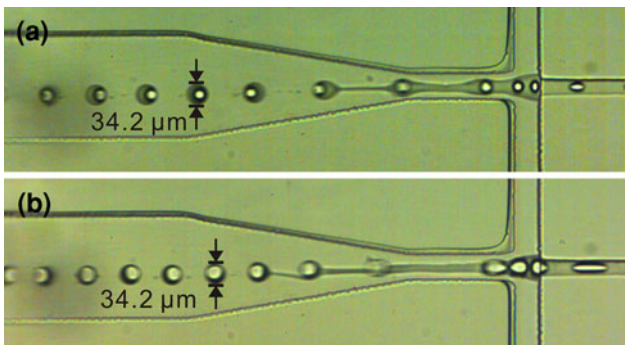

Fig. 4 Size control of the liquid core by flow rates. **a** Formation of the double-emulsion droplets with the liquid cores of size 15.0 μm. $Q_i = 0.01$ mL h^{-1}, $Q_m = 0.05$ mL h^{-1} and $Q_o = 4$ mL h^{-1}. **b** Formation of the double-emulsion droplets with the liquid cores of size 23.3 μm. $Q_i = 0.03$ mL h^{-1}, $Q_m = 0.03$ mL h^{-1} and $Q_o = 4$ mL h^{-1}

3.2 Optical properties of QD-loaded liquid core

For the method of doping the QDs inside the polymer microparticles, the quantum efficiencies of QDs decrease after being doped inside the solid-state polymer matrix (Sheng et al. 2006). We loaded the QDs in the liquid cores of microcapsules to maintain their original characteristics. The suspension medium of QDs in the liquid core remains the same as deionized water after the microcapsule formation. The UV-induced polymerization of ETPTA avoids the longtime heating that is required in doping the QDs in the solid-state polymer matrix by thermal polymerization or solvent removal. This longtime heating may reduce the QD photoluminescence intensities significantly. Although the UV-induced polymerization is an exothermal reaction, the continuing aqueous outer-phase flow can cool down the cured polymer shells immediately. Under UV illumination, the QD-loaded liquid cores show highly contrasted bright spots in their fluorescent micrograph, as shown in Fig. 7a. The fluorescence intensities across a microcapsule along line A–A' in Fig. 7b follows an intense parabola profile at its central core area and indicates that the ETPTA shell has a low autofluorescence. The autofluorescence of the cured ETPTA is about 4 % of the fluorescence intensity of the liquid core loaded with the QDs emitting at 600 nm in concentration of 0.5 μM. The fluorescence intensities of QD-loaded liquid cores are linearly proportional to the molar concentration of QDs in the liquid cores as shown in Fig. 8. The concentration interval of 0.1 μM is high enough to create a discernible intensity level for the QDs emitting at 600 nm. The fluorescence intensities of the QD-loaded liquid cores were highly

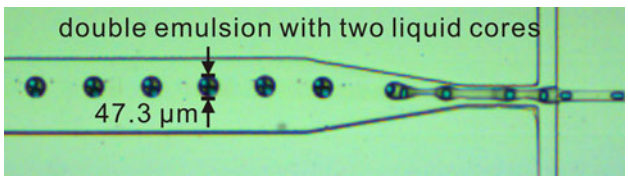

Fig. 5 Formation of the double-emulsion droplets with two liquid cores. $Q_i = 0.02$ mL h^{-1}, $Q_m = 0.07$ mL h^{-1} and $Q_o = 3$ mL h^{-1}

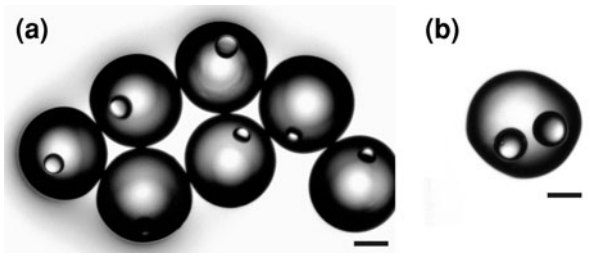

Fig. 6 **a** Bright-field micrograph of the monodispersed microcapsules with the liquid cores in two different sizes. **b** Bright-field micrograph of a microcapsule with two liquid cores. All the *scale bars* are 10 μm in length

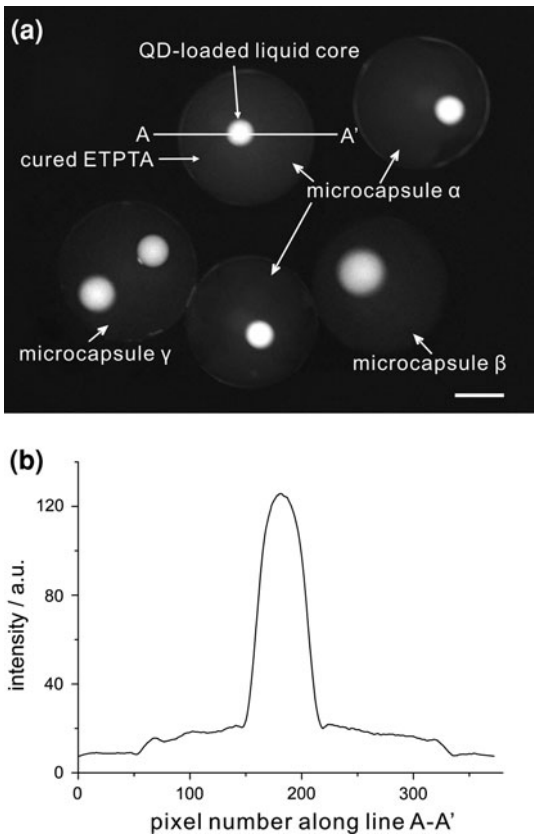

Fig. 7 **a** Fluorescent micrograph of the microcapsules. The liquid cores contain the QDs emitting at 600 nm. Each microcapsules α contains one small core. Each microcapsule β contains one big core. Each microcapsule γ contains two cores. The *scale bar* is 10 μm in length. **b** Fluorescence intensities across a microcapsule α along line A–A' follows a parabola profile

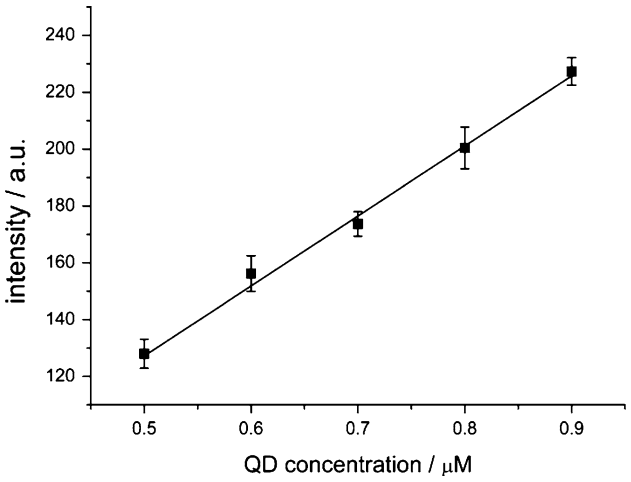

Fig. 8 Fluorescence intensities of the QD-loaded liquid cores as a function of the concentrations of QDs emitting at 600 nm in the liquid cores. The fluorescence intensities of the QD-loaded liquid cores are linearly proportional to the concentrations of the QDs in the liquid cores

repeatable for an identical batch of microcapsules and unchanged when the microcapsules were suspended in water, ethanol or PBS buffer.

It should be noted that the possibility of distance-depended FRET between the QDs of different colors increases with the total concentration of the QDs in the liquid core. We made five batches of microcapsules containing five different QD-loaded liquid cores to investigate this issue. The five aqueous QD mixtures to form the liquid cores were prepared by mixing the QDs with the emission peaks at 550 and 600 nm, respectively. The concentrations of the QDs emitting at 550 nm increased from 1 to 5 μM with an increment of 1 μM for the five QD mixtures. The concentrations of the QDs emitting at 600 nm were 0.5 μM constantly. The fluorescence intensities of the liquid cores at 550 and 600 nm were recorded as a bar chart in Fig. 9. The linear model fits the fluorescence intensities of the liquid cores at 550 and 600 nm with adjusted coefficients of determination (adjusted R^2) of 0.98 and 0.99, respectively, which indicates that the fluorescence intensities of liquid cores keep the linear relation with the QD concentrations in the liquid cores. The slightly linear increments of the fluorescence intensities of the liquid cores at 600 nm were attributed to the spectral overlapping from the QDs emitting at 550 nm in increasing concentrations. No obvious interference of photoluminescence emissions between the QDs with the two emission peaks was observed when the total concentration of the QDs was less than 5.5 μM. The fluorescent profile used to identify the barcode has a one-to-one correspondent relation to the composition of the QD mixture in the liquid core. This allows the barcode formation to be highly simplified as a multiplexing process for the QD emission peaks and concentrations in the liquid core, which does not require the interrogation of the specificity of the fluorescent profile for each QD liquid-core barcode. The fluorescence profiles of the QD barcodes in the microcapsules can be predefined directly by the compositions of the QD mixtures in the liquid cores.

3.3 Barcode formation and identification

Previous methods to identify the QD barcodes use spectrometers (Han et al. 2001) or flow cytometers (Giri et al. 2011) to record the fluorescent spectra or intensities of the QD-incorporated microparticles. We proposed a simple image-based decoding method for our liquid-core barcodes by capturing the fluorescent micrographs of the microcapsules at the respective QD emission peaks. We made a batch of barcoded microcapsules, in which the QD mixture in the liquid cores consisted of the QDs emitting at 550, 600 and 650 nm in concentration of 0.3, 0.2 and 0.1 μM, respectively. Three other batches of microcapsules containing the single-color QDs emitting at these three

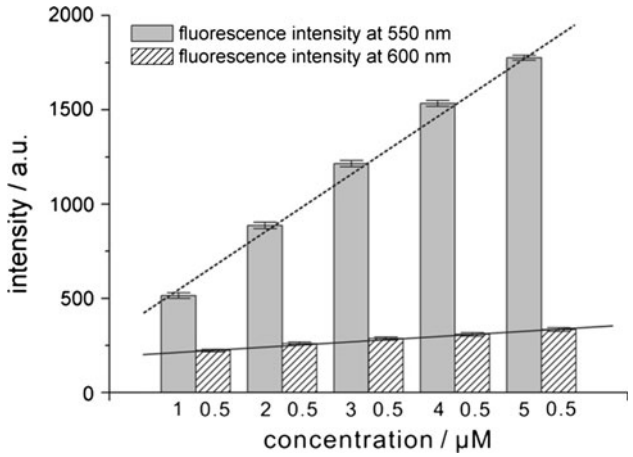

Fig. 9 *Bar chart* of the fluorescence intensities of the liquid cores containing five different QD mixtures which are prepared by mixing the QDs with emission *peaks* at 550 and 600 nm, respectively. The concentrations of QDs emitting at 550 nm increase from 1 to 5 μM with an increment of 1 μM for the five QD mixtures. The concentrations of the QDs emitting at 600 nm are 0.5 μM constantly. The *dashed line* and *solid line* are the linear fitting lines of the fluorescence intensities of liquid cores at 550 and 600 nm, respectively. No interference of photoluminescence emissions between the QDs with these two different emission peaks was observed when their total concentration was less than 5.5 μM

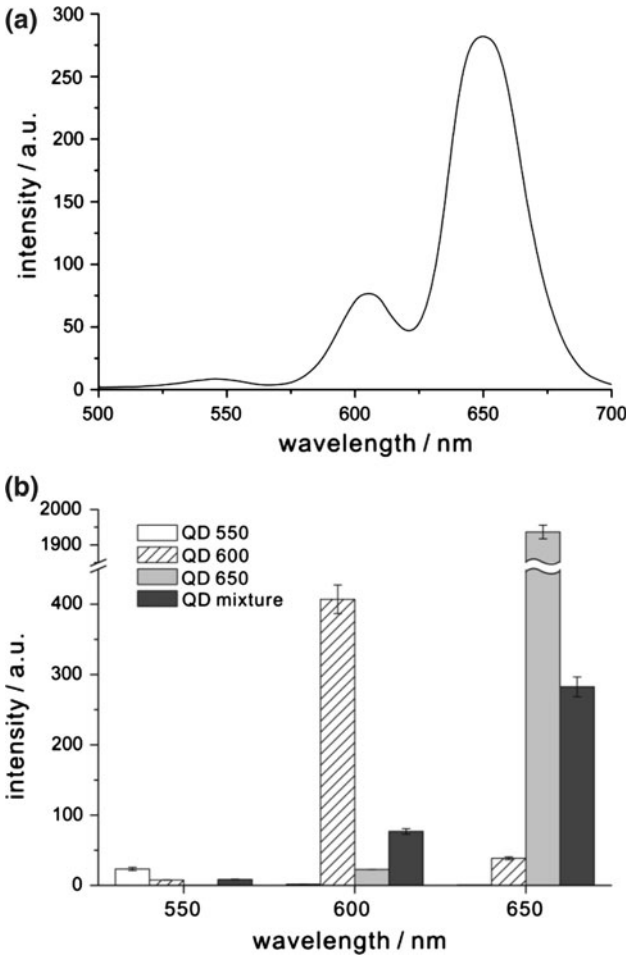

Fig. 10 **a** Fluorescent spectrum of the encoded microcapsule with the liquid core containing a QD mixture prepared by the QDs emitting at 550, 600 and 650 nm in concentrations of 0.3, 0.2 and 0.1 μM, respectively. **b** *Bar chart* of fluorescent intensity of the encoded microcapsule and the intensity-reference microcapsules

wavelengths in concentration of 1 μM were also made as intensity references. When the previous spectrum-based decoding method is used to identify this barcode, the fluorescent spectrum of this encoded microcapsule is recorded as shown in Fig. 10a. This spectrum-recoding process is relatively time-consuming, which requires about 7 ~ 8 min by hyperspectral imaging. In addition, the decoding process requires a deconvolution algorithm to separate the individual emission spectra of each color QDs from the overlapped spectrum (Lee et al. 2007). For our image-based decoding method, the fluorescence intensities of the barcoded microcapsule and the intensity-reference microcapsules at the three QD emission peaks were recorded as a bar chart in Fig. 10b. The composition of the QD mixture in the barcoded microcapsule, which is also used as the barcode, can be calculated easily according to these intensity-reference microcapsules. The calculated composition of the QD mixture is 0.31, 0.18 and 0.14 μM for the QDs emitting at 550, 600 and 650 nm, respectively. The relatively large error for the concentration of the QDs emitting at 650 nm may come from the variations of QD photoluminescence intensities and instrumental errors (Han et al. 2001), which causes the actual number of discernible barcodes to be less than the theoretical estimation of $(n^m\text{-}1)$ (n is the number of intensity levels and m is the number of colors). Here, the image-based decoding method shows its advantage in enhancing the coding capacity. Besides the fluorescent profiles, the fluorescent micrograph of the microcapsules can provide the graphical information of the sizes and numbers of the QD-loaded liquid cores in individual microcapsules, as shown in Fig. 7a. The graphical information of the liquid cores offers another dimension to form the barcodes, which can increase the coding capacity by at least one order of magnitude.

4 Conclusions

In summary, we reported new QD barcodes made by loading QDs in the liquid cores of the monodispersed microcapsules. Since the QDs in the liquid cores maintain their original characteristics, especially the linear relation between photoluminescence intensity and concentration, the barcode formation can be simplified as a multiplexing process for the QD emission peaks and concentrations in the liquid cores. The fluorescent profiles used to identify

the barcodes can be predefined directly by the compositions of QD mixtures before the formation of barcodes. In addition, the graphical information from the micrographs of the microcapsules about the sizes and numbers of the QD-loaded liquid cores further enhances the coding capacity. The barcodes of the microcapsules are formed by combinations of the fluorescent profiles of the QD-loaded liquid cores and the graphical information of the sizes and numbers of the liquid cores, which can be identified easily from the fluorescent micrographs of these microcapsules. The microfluidic method we presented can form the QD-barcoded microcapsules in small sizes of $\sim$30 μm, which is necessary for the barcodes to conduct the multiplexed assays in small-volume samples (Braeckmans and De Smedt 2010). These small barcoded microcapsules having stable fluorescent profiles in different bioassay buffers can be used as a platform for various high-throughput screening applications.

Acknowledgments Bo Wu would like to acknowledge the Ph.D. scholarship from Nanyang Technological University.

References

Birtwell S, Morgan H (2009) Microparticle encoding technologies for high-throughput multiplexed suspension assays. Integr Biol 1(5–6):345–362. doi:10.1039/b905502a

Birtwell SW, Galitonov GS, Morgan H, Zheludev NI (2008) Superimposed nanostructured diffraction gratings as high capacity barcodes for biological and chemical applications. Optics Commun 281(7):1789–1795. doi:10.1016/j.optcom.2007.04.066

Braeckmans K, De Smedt SC (2010) Colour-coded microcarriers made to move. Nat Mater 9(9):697–698. doi:10.1038/nmat2836

Cederquist KB, Dean SL, Keating CD (2010) Encoded anisotropic particles for multiplexed bioanalysis. Wiley Interdiscip Rev-Nanomed Nanobiotechnol 2(6):578–600. doi:10.1002/wnan.96

Dejneka MJ, Streltsov A, Pal S, Frutos AG, Powell CL, Yost K, Yuen PK, Muller U, Lahiri J (2003) Rare earth-doped glass microbarcodes. Proc Natl Acad Sci USA 100(2):389–393. doi:10.1073/pnas.0236044100

Eastman PS, Ruan WM, Doctolero M, Nuttall R, De Feo G, Park JS, Chu JSF, Cooke P, Gray JW, Li S, Chen FQF (2006) Qdot nanobarcodes for multiplexed gene expression analysis. Nano Lett 6(5):1059–1064. doi:10.1021/nl060795t

Fournier-Bidoz S, Jennings TL, Klostranec JM, Fung W, Rhee A, Li D, Chan WCW (2008) Facile and rapid one-step mass preparation of quantum-dot barcodes. Angew Chem-Int Edit 47(30):5577–5581. doi:10.1002/anie.200800409

Fulton RJ, McDade RL, Smith PL, Kienker LJ, Kettman JR (1997) Advanced multiplexed analysis with the FlowMetrix(TM) system. Clin Chem 43(9):1749–1756

Gao XH, Nie SM (2004) Quantum dot-encoded mesoporous beads with high brightness and uniformity: rapid readout using flow cytometry. Anal Chem 76(8):2406–2410. doi:10.1021/ac0354600

Giri S, Li DW, Chan WCW (2011) Engineering multifunctional magnetic-quantum dot barcodes by flow focusing. Chem Commun 47(14):4195–4197. doi:10.1039/c0cc05336h

Han MY, Gao XH, Su JZ, Nie S (2001) Quantum-dot-tagged microbeads for multiplexed optical coding of biomolecules. Nat Biotechnol 19(7):631–635

Hayward TJ, Hong B, Vyas KN, Palfreyman JJ, Cooper JFK, Jiang Z, Jeong JR, Llandro J, Mitrelias T, Bland JAC, Barnes CHW (2010) Magnetic micro-barcodes for molecular tagging applications. J Phys D Appl Phys 43(17):175001. doi:10.1088/0022-3727/43/17/175001

Kellar KL, Iannone MA (2002) Multiplexed microsphere-based flow cytometric assays. Exp Hematol 30(11):1227–1237. doi:10.1016/s0301-472x(02)00922-0

Lee JA, Mardyani S, Hung A, Rhee A, Klostranec J, Mu Y, Li D, Chan WCW (2007) Toward the accurate read-out of quantum dot barcodes: design of deconvolution algorithms and assessment of fluorescence signals in buffer. Adv Mater 19(20):3113–3118. doi:10.1002/adma.200701955

Lee JB, Roh YH, Um SH, Funabashi H, Cheng WL, Cha JJ, Kiatwuthinon P, Muller DA, Luo D (2009) Multifunctional nanoarchitectures from DNA-based ABC monomers. Nat Nanotechnol 4(7):430–436. doi:10.1038/nnano.2009.93

Lee H, Kim J, Kim H, Kwon S (2010) Colour-barcoded magnetic microparticles for multiplexed bioassays. Nat Mater 9(9):745–749. doi:10.1038/nmat2815

Nicewarner-Peña SR, Freeman RG, Reiss BD, He L, Peña DJ, Walton ID, Cromer R, Keating CD, Natan MJ (2001) Submicrometer metallic barcodes. Science 294(5540):137–141. doi:10.1126/science.294.5540.137

Nie ZH, Xu SQ, Seo M, Lewis PC, Kumacheva E (2005) Polymer particles with various shapes and morphologies produced in continuous microfluidic reactors. J Am Chem Soc 127(22):8058–8063. doi:10.1021/ja042494w

Okushima S, Nisisako T, Torii T, Higuchi T (2004) Controlled production of monodisperse double emulsions by two-step droplet breakup in microfluidic devices. Langmuir 20(23):9905–9908. doi:10.1021/la0480336

Pregibon DC, Toner M, Doyle PS (2007) Multifunctional encoded particles for high-throughput biomolecule analysis. Science 315(5817):1393–1396. doi:10.1126/science.1134929

Rauf S, Glidle A, Cooper JM (2009) Production of quantum dot barcodes using biological self-assembly. Adv Mater 21(40):4020–4024. doi:10.1002/adma.200900223

Schneider MH, Willaime H, Tran Y, Rezgui F, Tabeling P (2010) Wettability patterning by UV-initiated graft polymerization of poly(acrylic acid) in closed microfluidic systems of complex geometry. Anal Chem 82(21):8848–8855. doi:10.1021/ac101345m

Sheng WC, Kim S, Lee J, Kim SW, Jensen K, Bawendi MG (2006) In situ encapsulation of quantum dots into polymer microspheres. Langmuir 22(8):3782–3790. doi:10.1021/la0519731

Su X, Zhang J, Sun L, Koo T-W, Chan S, Sundararajan N, Yamakawa M, Berlin AA (2004) Composite organic−inorganic nanoparticles (COINs) with chemically encoded optical signatures. Nano Lett 5(1):49–54. doi:10.1021/nl0484088

Utada AS, Lorenceau E, Link DR, Kaplan PD, Stone HA, Weitz DA (2005) Monodisperse double emulsions generated from a microcapillary device. Science 308(5721):537–541. doi:10.1126/science.1109164

Vaidya SV, Gilchrist ML, Maldarelli C, Couzis A (2007) Spectral bar coding of polystyrene microbeads using multicolored quantum dots. Anal Chem 79(22):8520–8530. doi:10.1021/ac0710533

Wang DY, Rogach AL, Caruso F (2002) Semiconductor quantum dot-labeled microsphere bioconjugates prepared by stepwise self-assembly. Nano Lett 2(8):857–861. doi:10.1021/nl025624c

Wilson R, Cossins AR, Spiller DG (2006) Encoded microcarriers for high-throughput multiplexed detection. Angew Chem-Int Edit 45(37):6104–6117. doi:10.1002/anie.200600288

Yu WW, Qu LH, Guo WZ, Peng XG (2003) Experimental determination of the extinction coefficient of CdTe, CdSe, and CdS nanocrystals. Chem Mat 15(14):2854–2860. doi:10.1021/cm034081k

Zhao Y, Zhao X, Hu J, Xu M, Zhao W, Sun L, Zhu C, Xu H, Gu Z (2009) Encoded porous beads for label-free multiplex detection of tumor markers. Adv Mater 21(5):569–572. doi:10.1002/adma.200802339

Zhao YJ, Shum HC, Chen HS, Adams LLA, Gu ZZ, Weitz DA (2011) Microfluidic generation of multifunctional quantum dot barcode particles. J Am Chem Soc 133(23):8790–8793. doi:10.1021/ja200729w